Technical Note

Deformation of Reef Breakwaters and Wave Transmission

Nobuhisa Kobayashi, M.ASCE[1]; Jill Pietropaolo[2]; and Jeffrey A. Melby, M.ASCE[3]

Abstract: The risk-based design of a reef breakwater requires the prediction of the temporal variations of the damage and wave transmission coefficient during storms. The cross-shore numerical model is extended to the landward zone of the wave transmission. The extended model is compared with 148 tests for a reef breakwater with a narrow crest at or above the still water level where the narrow crest was lowered by wave action. The model is also compared with an experiment on a wide-crested submerged breakwater in which the crest height increased during 20-h wave action. The damage, crest height, and wave transmission coefficient are predicted reasonably well; however, the damaged profile is not predicted accurately. **DOI: 10.1061/(ASCE)WW.1943-5460.0000180.**

CE Database subject headings: Reefs; Breakwaters; Damage; Wave overtopping; Numerical models; Wave actions; Coefficients; Wave crest.

Author keywords: Reef breakwaters; Rubble mounds; Damage; Wave overtopping; Wave transmission.

Introduction

A reef breakwater is a low-crested stone structure constructed for beach stabilization and shore protection (Ahrens 1989). The reef breakwater is designed to allow wave overtopping and transmission as well as some stone movement and structure deformation as long as the shore protection requirement is satisfied. This design flexibility may reduce the structure cost; however, the hydraulic and structural performance of the reef breakwater must be predicted reliably.

Empirical formulas can be used to predict wave transmission over and through low-crested structures with no deformation (Goda and Ahrens 2008). Wave transmission is sensitive to the crest height of the reef breakwater relative to the still water level (SWL). Ahrens (1989) conducted laboratory tests for a trapezoidal reef breakwater with a crest width of three stone diameters, having seaward and landward slopes of 1 on 1.5, and proposed an empirical formula to predict the crest height of the stabilized reef breakwater for this specific initial profile. Vidal et al. (1992) conducted a laboratory experiment and showed the significant influence of the crest height of a low-crested breakwater on the stone stability on its seaward slope, crest, and landward slope of the low-crested breakwater. To date, the stability and damage progression on a low-crested breakwater of arbitrary geometry cannot be predicted reliably because available data sets are limited in comparison with the number of data sets used for the development of stability and damage formulas for conventional rubble mound breakwaters with little or no wave overtopping (e.g., Melby and Kobayashi 2011).

Kobayashi et al. (2010) expanded the cross-shore numerical model, *CSHORE*, to predict damage progression of a stone armor layer on a conventional rubble mound breakwater. This paper extends the numerical model to the landward zone of the wave transmission to predict the deformation of a reef breakwater under irregular wave action. The extended model is compared with 148 tests by Ahrens (1989), in which a reef breakwater with a narrow crest at or above the SWL was exposed to approximately 4,000 waves in each test. The narrow crest was lowered because of the landward and seaward stone displacement on the steep (1/1.5) slopes in these tests. The numerical model is evaluated using the measured damage, lowered crest height, and wave transmission coefficient for each test. The numerical model is also compared with the experiment by Ota et al. (2006) in which a wide-crested submerged reef breakwater was deformed by 20 h of wave action. The landward stone movement on the wide crest resulted in the increase of the crest height and the decrease of the wave transmission coefficient.

Numerical Model

An emerged reef breakwater consisting of a homogeneous pile of stones is depicted in Fig. 1. Alongshore uniformity and normally incident waves are assumed. The cross-shore coordinate x is positive onshore with $x = 0$ at the offshore location of the incident irregular wave measurement. The landward end location of $x = x_m$ corresponds to the location of the transmitted wave measurement. The vertical coordinate z is positive upward with $z = 0$ at the SWL. The upper and lower boundaries of the stone breakwater are located at $z = z_b(x)$ and $z_p(x)$, respectively, where the lower boundary is assumed to be impermeable and $z_b(x) = z_p(x)$ seaward and landward of the breakwater. The horizontal SWL and $z_b(x)$ intersect at $x = x_{SWL}$ and x_s, where the hydrodynamic model by Kobayashi et al. (2010) was limited to the seaward wet zone of $x < x_{SWL}$ and the wet and dry zones of $x_{SWL} < x < x_s$. The crest is located at $x = x_c$ corresponding to the most landward location of the maximum $z_b(x)$. The hydrodynamic model computes the wave overtopping rate q_o as the sum of the volume fluxes q and q_p at $x = x_c$ above and inside the porous breakwater, respectively. The computation in the wet and dry zones is limited to the zone of $x < x_d$, where the computed mean

[1]Professor and Director, Center for Applied Coastal Research, Univ. of Delaware, Newark, DE 19716 (corresponding author). E-mail: nk@udel.edu

[2]M.S. Student, Dept. of Civil and Environmental Engineering, Univ. of Delaware, Newark, DE 19716.

[3]Research Hydraulic Engineer, U.S. Army Engineer Research and Development Center, 3909 Halls Ferry Rd., Vicksburg, MS 39180-6199.

Note. This manuscript was submitted on April 9, 2012; approved on July 23, 2012; published online on July 28, 2012. Discussion period open until December 1, 2013; separate discussions must be submitted for individual papers. This technical note is part of the ***Journal of Waterway, Port, Coastal, and Ocean Engineering***, Vol. 139, No. 4, July 1, 2013. ©ASCE, ISSN 0733-950X/2013/4-336–340/$25.00.

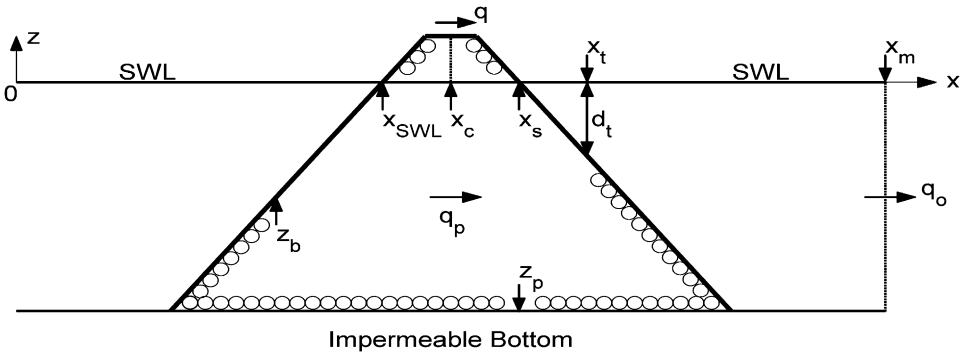

Fig. 1. Wave overtopping and transmission through emerged reef breakwater

water depth $\overline{h}$ exceeds 0.01 cm. The computation end point x_d is located between x_{SWL} and x_s, as explained subsequently. If the crest of the deformed breakwater under wave action becomes submerged, then no wet and dry zones exist and the hydrodynamic model for the wet zone is the same as that developed for a submerged porous breakwater by Kobayashi et al. (2007).

The hydrodynamic model by Kobayashi et al. (2010) is extended to the landward wet zone of $x > x_s$. For low-crested structures, the computation in the wet and dry zone normally ends at $x = x_s$ and $x_d = x_s$. However, this is not the case for small wave heights and periods. If $x_d < x_s$, then the overtopping flow does not reach the landward wet zone and no water is present in the zone of $x_d < x < x_s$ above $z_b(x)$. If $x_d \geq x_c$, then the wave overtopping rate q_o computed at x_c is assumed to determine the volume flux $q_p = q_o$ in the zone of $x_d < x < x_s$ below $z_b(x)$. If $x_d < x_c$, then wave runup on the seaward slope does not reach the crest of the structure. In this case of no overtopping, the volume flux q_p in the zone of $x_d < x < x_s$ is estimated using the formula based on the water level difference between the two points at $x = x_d$ above the SWL and x_s at the SWL by Kobayashi and de los Santos (2007).

In the landward wet zone, plunging water at $x = x_s$ produces complex hydrodynamics in the transition zone of $x_s < x < x_t$ in Fig. 1, where the still water depth d_t is specified to estimate the landward location of $x = x_t$. The mean water depth $\overline{h}_s$ and the free surface standard deviation σ_s at $x = x_s$ are computed by the hydrodynamic model in the wet and dry zones. The ratio of $d_t/\overline{h}_s$ is the jump of the water depth in the transition zone. The assumption of $(d_t/\overline{h}_s) = 10$ is made in the following computations. The computed results are found to be insensitive to this depth ratio on the order of 10. If $x_d < x_s$, then $\overline{h}_s = 0$ and $\sigma_s = 0$. Under these conditions, the volume flux $q_p = q_o$ at $x = x_s$ through the porous structure is assumed to generate transmitted waves. For this case of no plunging water, $d_t = 1$ cm is used for the seepage flow transition below the SWL.

In the zone of $x > x_t$, use is made of the following two equations based on linear wave theory (Kobayashi et al. 2007):

$$\sigma_\eta \sigma_U + \overline{h}\,\overline{U} + q_p = q_o; \quad \sigma_U = C\sigma_\eta/\overline{h} \quad \text{for } x > x_t \qquad (1)$$

where σ_η = standard deviation of the free surface elevation η above the SWL related to the spectral significant wave height $H_{mo} = 4\sigma_\eta$; σ_U = standard deviation of the depth-averaged horizontal velocity U; $\overline{h}$ = mean water depth given by $\overline{h} = (\overline{\eta} - z_b)$ with $\overline{\eta}$ = mean water level above the SWL; $\overline{U}$ = wave-induced current velocity; q_p = volume flux inside the porous layer with its thickness $h_p = (z_b - z_p)$; q_o = wave overtopping rate including the seepage rate computed by the hydrodynamic model in the wet and dry zones; and C = wave phase velocity approximated as $C = (g\overline{h})^{0.5}$ with g = gravitational acceleration. The probability distributions of η and U are assumed to be Gaussian in the wet zone and the term $\sigma_\eta\sigma_U$ in Eq. (1) is the wave-induced onshore flux above z_b. The volume flux at the landward boundary $x = x_m$ is assumed to be the wave overtopping rate q_o as indicated in Fig. 1. This assumption may be reasonable for the emerged reef experiment by Ahrens (1987), where water was allowed to flow landward; however, some water could have returned seaward especially after the reef was submerged. For the submerged reef experiment by Ota et al. (2006), $q_o = 0$ at $x = x_m$ because of no flux at the end of their flume experiment. The wave transmission coefficient K_t is defined as the ratio between $H_{mo} = 4\sigma_\eta$ at $x = x_m$ and H_{mo} at $x = 0$. The volume flux q_p through the thickness h_p for the zone of $x > x_s$ is estimated assuming that the discharge velocity (q_p/h_p) remains the same as the discharge velocity at $x = x_s$ computed by the hydrodynamic model in the wet and dry zones. The flux q_p decreases landward with the decrease of h_p.

Eq. (1) is used to obtain σ_η, $\overline{\eta} = (\overline{h} + z_b)$, σ_U, and $\overline{U}$, where σ_U and $\overline{U}$ are required for the prediction of the stone transport rate, as explained subsequently. If $x_d = x_s$, then plunging water occurs at $x = x_s$ and the values of $\sigma_\eta = \sigma_s$, $\overline{h} = \overline{h}_s$, σ_U, and $\overline{U}$ at $x = x_s$ with $z_b = 0$ are known. It is simply assumed that $\sigma_\eta = \sigma_s$ and $\overline{\eta} = \overline{h}_s$ for $x > x_s$. Eq. (1) is used to obtain σ_U and $\overline{U}$ for $x \geq x_t$. The values of σ_U and $\overline{U}$ in the transition zone are interpolated linearly between those at $x = x_s$ and x_t. If $x_d < x_s$, then $\sigma_s = 0$ and $\overline{h}_s = 0$. The assumption of no wave setup $(\overline{\eta} = 0)$ for $x > x_s$ may be acceptable; however, the assumption of $\sigma_\eta = 0$ for $x > x_s$ implies no wave transmission through the porous structure. The assumption of $\overline{U} = 0$ for $x > x_s$ is made instead to obtain σ_η and σ_U using Eq. (1). The values of σ_η and σ_U in the transition zone are interpolated linearly between those at $x = x_s$ and x_t.

The volumetric rate q_b of stone transport in the computation domain of $0 \leq x \leq x_m$ is estimated using the formula for bed load by Kobayashi et al. (2010). This formula predicts onshore stone movement on the bottom located at $z = z_b(x)$ as long as the local bottom slope $(\partial z_b/\partial x)$ is less than approximately 1/3. The stone movement on the steep seaward slope exceeding 1/3 is offshore. The formula for q_b accounts for limited stone availability, and $q_b = 0$ if $z_b = z_p$. The input empirical parameters in the subsequent computations are taken to be the same as those used by Kobayashi et al. (2010) except for the critical stability number N_c of the order of unity, which is related to the critical threshold velocity of stone movement. The calibrated value of N_c for three tests of a conventional rubble mound breakwater was 0.6 or 0.7. For the present comparisons for low-crested and submerged reef breakwaters,

J. Waterway, Port, Coastal, Ocean Eng. 2013.139:336-340.

use is made of $N_c = 1.0$, where the critical velocity is proportional to $\sqrt{N_c}$. The increase of N_c reduces the deformation of reef breakwaters. The temporal change of the bottom elevation z_b is computed using the conservation equation of the stone volume where the stone porosity is assumed to remain constant. The computation time is of the order of 10^{-3} of the duration of a laboratory test.

Comparison with Narrow Reef Data

Ahrens (1987, 1989) conducted reef breakwater model tests in a channel of 61-cm width constructed in a wave tank that was 1.2-m high, 4.6-m wide, and 42.7-m long. A reef breakwater with a crest width of three stone diameters was constructed on a horizontal bottom. The seaward and landward slopes were 1/1.5. The numerical model is compared with five sets consisting of 148 tests as summarized in Table 1. The nominal stone diameter D_{n50} is defined as $D_{n50} = (M_{50}/\rho_s)^{1/3}$ with M_{50} = median stone mass and ρ_s = stone density. Two sizes of stone were used in these tests. For the smaller stone, $M_{50} = 17$ g, $\rho_s = 2.63$ g/cm^3, and $n_p = 0.45$, where n_p = porosity of the stone structure. For the larger stone, $M_{50} = 71$ g, $\rho_s = 2.83$ g/cm^3, and $n_p = 0.44$. The still water depth d_s above the horizontal bottom was 25 or 30 cm. The initial reef crest height h_c' above the horizontal bottom was near the SWL for Set 1 and above the SWL for Sets 2–5. The incident waves for each test were measured approximately 3-m seaward of the reef breakwater. The spectral significant wave height H_{mo} was in the range of 1.7–11.6 cm. The spectral peak period T_p was in the range of 1.3–2.6 s. The duration of each test was approximately $3{,}750T_p$. The crest of the reef breakwater was lowered because of the onshore stone movement on the crest and landward slope and the offshore stone movement on the seaward slope during each test. The eroded area A_e and the crest height h_c at the end of each test were measured and reported by Ahrens (1987). The transmitted waves were measured about 1-m landward of the breakwater and the transmitted significant wave height was reported for each test.

Fig. 2 compares the measured and computed damage S defined as $S = (A_e/D_{n50}^2)$. The root-mean-square relative error E is calculated separately for each test, where E is the standard deviation of the relative error given by $(C_i - M_i)/M_i$ with C_i and M_i = computed and measured values for the ith test in each set. The perfect agreement and deviations of a factor of 2 are indicated by a solid line and dashed lines, respectively. The numerical model tends to underpredict S for Set 5 and overpredict S for Set 7. The value of E for Set 9 is large because the measured S for six tests out of 13 tests in Set 9 was less than unity and the very small damage is difficult to predict accurately. The agreement could be improved by calibrating the critical stability number N_c for each set instead of $N_c = 1.0$ for all sets; however, the overall agreement of a factor of about 2 is similar to that of the empirical damage prediction for conventional rubble mound breakwaters (Melby and Kobayashi 2011).

Table 1. Summary of Narrow Reef Experiment by Ahrens (1987)

Set	Number of tests	D_{n50} (cm)	d_s (cm)	h_c' (cm)	H_{mo} (cm)	T_p (s)
1	27	1.86	25	24.1–24.8	2.9–10.2	1.4–2.5
3	29	1.86	25	28.7–29.4	2.6–9.6	1.4–2.6
5	41	1.86	25	34.4–35.3	1.8–9.1	1.3–2.5
7	38	2.93	25	31.2–31.8	1.7–9.2	1.4–2.6
9	13	2.93	30	31.6–31.8	5.2–11.6	1.4–2.6

Fig. 3 compares the measured and computed crest heights h_c normalized by d_s at the end of each test, where $(h_c/d_s) < 1$ implies the reef crest below the SWL after the test completion. The dashed lines in Fig. 3 indicate 20% deviations from the solid line of perfect agreement. The agreement appears better in Fig. 3 than in Fig. 2 because the crest height is hardly affected by the small damage S. The numerical model tends to overpredict (h_c/d_s) for tests with the measured $(h_c/d_s) < 1$ in Sets 3 and 5. This overprediction of the submerged crest height may be caused by the artificial separation of the various zones relative to the SWL. For practical applications, the temporal water level variation may reduce the effect of this artificial separation.

Fig. 4 shows the measured and computed wave transmission coefficients, where the dashed lines indicate deviations of a factor of 2 from the solid line of perfect agreement. The data points with significant underprediction of K_t correspond to the tests with the incident wave height H_{mo} of the order of the nominal stone diameter D_{n50}. The numerical model does not account for discrete stone units and cannot predict the wave transmission through the width of several stone diameters. The data points with the computed $K_t \simeq 1.0$ correspond to the tests with $h_c/d_t \simeq 1.0$, in which the separation between the wet zone and the wet and dry zones in the numerical model becomes too artificial. Some of the disagreement

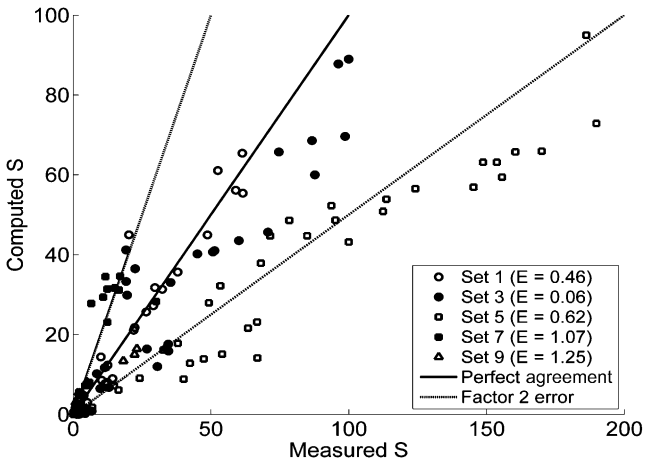

Fig. 2. Measured and computed damage S for narrow reefs

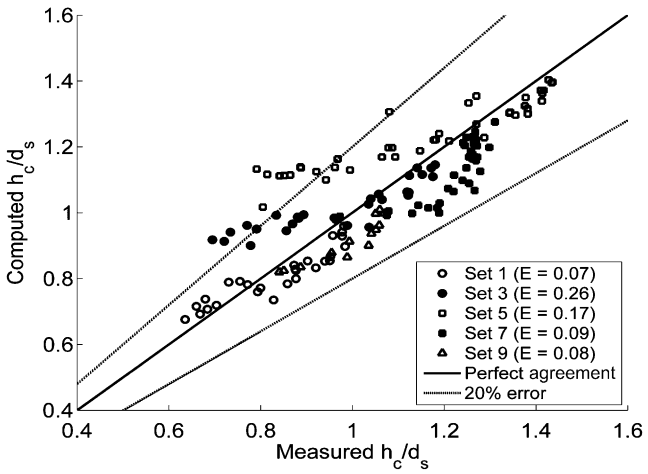

Fig. 3. Measured and computed crest heights for narrow reefs

J. Waterway, Port, Coastal, Ocean Eng. 2013.139:336-340.

in Fig. 4 arises from the disagreement in Fig. 3 because the wave transmission coefficient is sensitive to the crest height $(h_c - d_s)$ above the SWL. The overall agreement in Fig. 4 is no better than that of the empirical formula by Goda and Ahrens (2008), in which the measured values of h_c were used.

Comparison with Wide Submerged Reef Data

A number of wide submerged reef breakwaters were constructed in Japan. The design of these breakwaters was based on static stability criteria against design storm conditions. Ota et al. (2006) conducted an experiment to investigate the performance of such a breakwater against storm waves exceeding the design wave conditions. The experiment was conducted in a wave flume that was 29-m long, 0.5-m wide, and 0.75-m high. A reef breakwater was constructed of stone on a slope of 1/30. The nominal diameter and porosity of the stone were $D_{n50} = 2.52$ cm ($M_{50} = 42.8$ g and $\rho_s = 2.69$ g/cm^3) and $n_p = 0.5$. The crest width was 110 cm. The still water depths at the toe and on the crest were 22.2 and 5.5 cm, respectively. The seaward and landward slopes were 1/3 and 1/2, respectively. The incident waves were measured in a water depth of 50 cm on the horizontal bottom approximately 9.5-m seaward of the breakwater toe. The transmitted waves were measured 0.5-m landward of the breakwater heel. The breakwater was exposed to 60 bursts of wave action, where each burst lasted 20 min. The measured spectral period and spectral significant wave height were approximately 2.0 s and 11.5 cm.

The measured initial profile was smoothed before the computation because the numerical model does not account for discrete stone units. The measured and computed final profiles after the 20-h wave action are shown along with the smoothed initial profile in Fig. 5. The numerical model predicts the measured onshore stone movement and crest height increase; however, the shape of the deformed seaward slope is not predicted well. Fig. 6 shows the measured and computed temporal variations of the damage S for the 20-h duration. The damage progressed almost linearly with time, unlike conventional rubble mound breakwaters with little wave overtopping for which the damage progression was observed to slow down with time (Melby and Kobayashi 2011). Figs. 5 and 6 indicate that the damaged profile is harder to predict than the damaged area. Fig. 7 shows the measured and computed temporal variations of the wave transmission coefficient, which decreased with time because of the increase of the crest height. The numerical model initially underpredicted the wave transmission coefficient somewhat. The degree of the underprediction increased with time, perhaps because of the difference between the measured and computed crest shapes as shown in Fig. 5.

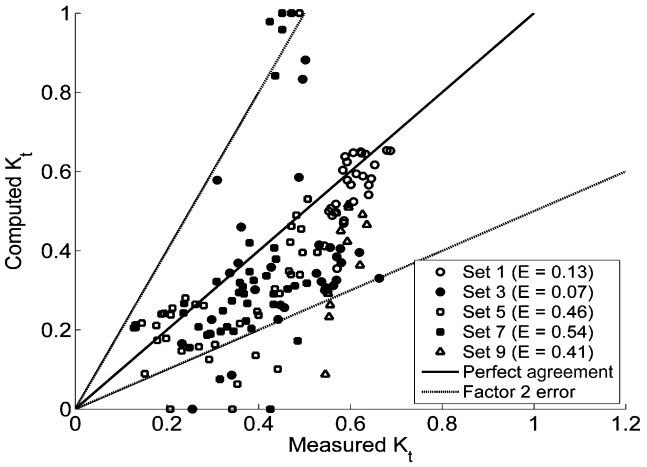

Fig. 4. Measured and computed wave transmission coefficients for narrow reefs

Conclusions

The deformation of a reef breakwater and the wave transmission landward of the deforming breakwater need to be predicted to perform the risk-based design of the breakwater. The cross-shore numerical model, *CSHORE*, is extended to the landward wet zone of wave transmission caused by wave overtopping over the breakwater and water volume flux through the porous breakwater. The extended model is compared with 148 tests by Ahrens (1989), where a reef breakwater with a narrow crest at or above the SWL was exposed to approximately 4,000 waves in each test. The numerical model is found to predict the damage and wave transmission coefficient within a factor of about 2 if the incident significant wave height is larger than the nominal stone diameter. The lowered crest height is predicted within errors of about 20%. The numerical model is also compared with the experiment by Ota et al. (2006), in which the crest height of a wide-crested submerged reef breakwater increased during 20-h wave action. The numerical model predicts the temporal variations of the damage and wave transmission coefficient fairly well; however, the damaged seaward profile of the breakwater is not predicted accurately. The

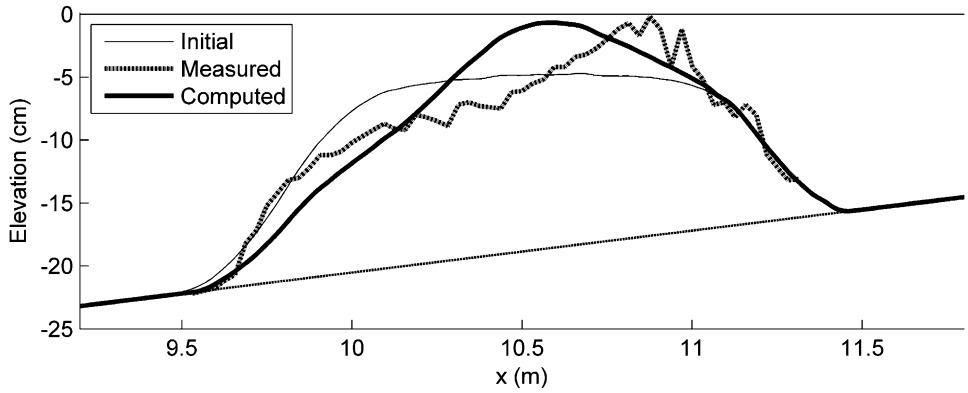

Fig. 5. Measured and computed deformed reef profiles atop the bottom slope after 20-h wave action

J. Waterway, Port, Coastal, Ocean Eng. 2013.139:336-340.

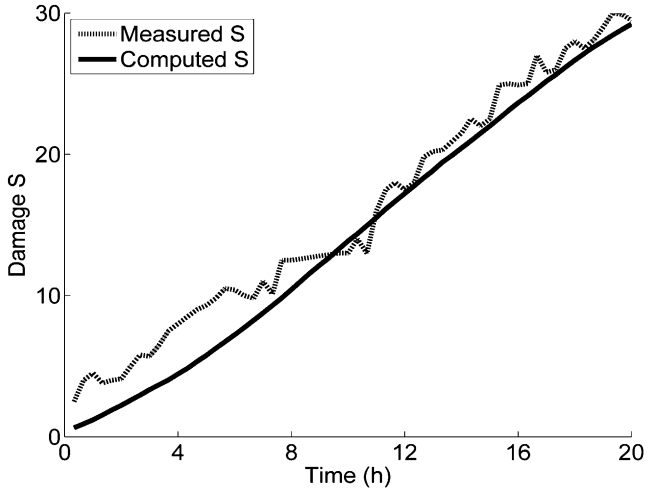

Fig. 6. Damage progression with time for a wide submerged reef

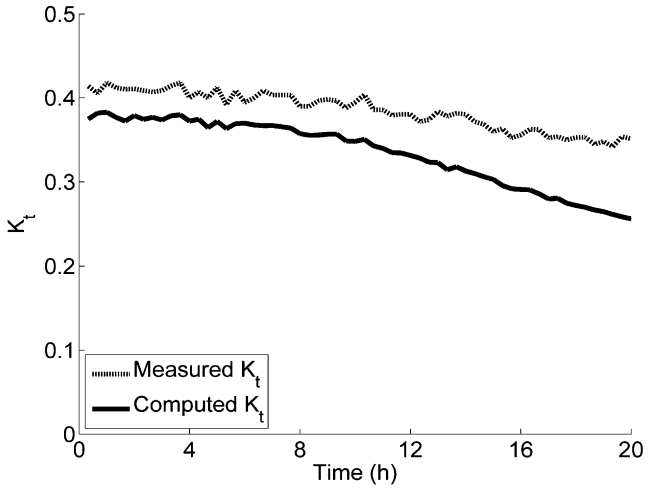

Fig. 7. Decrease of the wave transmission coefficient with time

errors of the numerical model will reduce the reliability of the risk-based design of the breakwater. To improve the extended model, detailed hydrodynamic measurements are required in the vicinity of the reef crest located near the SWL.

Acknowledgments

This study was partially supported by the U.S. Army Corps of Engineers Coastal and Hydraulics Laboratory under Contract No. W912HZ-11-P-0173 and by the EU THESEUS Project.

References

Ahrens, J. P. (1987). "Characteristics of reef breakwaters." *CERC Technical Rep. 87-17*, Coastal Engineering Research Center, Vicksburg, MS.

Ahrens, J. P. (1989). "Stability of reef breakwaters." *J. Waterway, Port, Coastal, Ocean Eng.*, 115(2), 221–234.

Goda, Y., and Ahrens, J. P. (2008). "New formulation of wave transmission over and through low-crested structures." *Proc., 31st Coastal Engineering Conf.*, World Scientific, Singapore, 3530–3541.

Kobayashi, N., and de los Santos, F. J. (2007). "Irregular wave seepage and overtopping of permeable slopes." *J. Waterway, Port, Coastal, Ocean Eng.*, 133(4), 245–254.

Kobayashi, N., Farhadzadeh, A., and Melby, J. A. (2010). "Wave overtopping and damage progression of stone armor layer." *J. Waterway, Port, Coastal, Ocean Eng.*, 136(5), 257–265.

Kobayashi, N., Meigs, L. E., Ota, T., and Melby, J. A. (2007). "Irregular breaking wave transmission over submerged porous breakwaters." *J. Waterway, Port, Coastal, Ocean Eng.*, 133(2), 104–116.

Melby, J. A., and Kobayashi, N. (2011). "Stone armor damage initiation and progression based on the maximum wave momentum flux." *J. Coastal Res.*, 27(1), 110–119.

Ota, T., Kobayashi, N., and Kimura, A. (2006). "Irregular wave transformation over deforming submerged breakwater." *Proc., 30th Coastal Engineering Conf.*, World Scientific, Singapore, 4945–4956.

Vidal, C., Losada, M. A., Medina, R., Mansard, E. P. D., and Gomez-Pina, G. (1992). "A numerical analysis for the stability of both low-crested and submerged breakwaters." *Proc., 23rd Coastal Engineering Conf.*, ASCE, Reston, VA, 1679–1692.

J. Waterway, Port, Coastal, Ocean Eng. 2013.139:336-340.